PCCP

PAPER

View Article Online
View Journal | View Issue

Cite this: *Phys. Chem. Chem. Phys.*, 2015, **17**, 18980

Hydrogen-bond acidity of ionic liquids: an extended scale†

Kiki A. Kurnia,[ab] Filipa Lima,[a] Ana Filipa M. Cláudio,[a] João A. P. Coutinho[a] and Mara G. Freire*[a]

One of the main drawbacks comprising an appropriate selection of ionic liquids (ILs) for a target application is related to the lack of an extended and well-established polarity scale for these neoteric fluids. Albeit considerable progress has been made on identifying chemical structures and factors that influence the polarity of ILs, there still exists a high inconsistency in the experimental values reported by different authors. Furthermore, due to the extremely large number of possible ILs that can be synthesized, the experimental characterization of their polarity is a major limitation when envisaging the choice of an IL with a desired polarity. Therefore, it is of crucial relevance to develop correlation schemes and *a priori* predictive methods able to forecast the polarity of new (or not yet synthesized) fluids. In this context, and aiming at broadening the experimental polarity scale available for ILs, the solvatochromic Kamlet–Taft parameters of a broad range of bis(trifluoromethylsulfonyl)imide-($[NTf_2]^-$)-based fluids were determined. The impact of the IL cation structure on the hydrogen-bond donating ability of the fluid was comprehensively addressed. Based on the large amount of novel experimental values obtained, we then evaluated COSMO-RS, COnductor-like Screening MOdel for Real Solvents, as an alternative tool to estimate the hydrogen-bond acidity of ILs. A three-parameter model based on the cation–anion interaction energies was found to adequately describe the experimental hydrogen-bond acidity or hydrogen-bond donating ability of ILs. The proposed three-parameter model is also shown to present a predictive capacity and to provide novel molecular-level insights into the chemical structure characteristics that influence the acidity of a given IL. It is shown that although the equimolar cation–anion hydrogen-bonding energies (E_{HB}) play the major role, the electrostatic-misfit interactions (E_{MF}) and van der Waals forces (E_{vdW}) also contribute, admittedly in a lower extent, towards the hydrogen-bond acidity of ILs. The new extended scale provided for the hydrogen-bond acidity of ILs is of high value for the design of new ILs for task-specific applications.

Received 28th May 2015,
Accepted 23rd June 2015

DOI: 10.1039/c5cp03094c

www.rsc.org/pccp

1. Introduction

Since the first report on water-stable ionic liquids (ILs),[1] these fluids have attracted large attention and shown tremendous growth in both academic and industrial studies. ILs are salts composed of large and bulky organic cations combined with either organic or inorganic anions, allowing a large part of them to remain liquid at temperatures close to room temperature. Aprotic ILs have appeared as major solvents to rival volatile organic compounds (VOCs) mainly due to their negligible vapour pressures under ambient conditions, preventing therefore evaporative losses to the environment – a fact which offers safety, ecological, and economic benefits. Other essential features connected to ILs include their broad liquidus temperature range, high chemical and thermal stabilities, and the ability to dissolve diverse types of solutes (*e.g.*, recalcitrant polymers such as cellulose and chitin).[2,3] Due to their outstanding features, ILs have been studied as more environmentally benign solvent media in a large number of applications, such as in organic and inorganic synthesis, catalysis, polymerization, and separation/extraction processes.[4–8] The motivation behind the booming research on ILs is not only a result of their excellent properties,[9] but also an outcome of their tuneable character. Their physicochemical properties can be tailored to suit a specific function by changing their ion chemical structures, including the incorporation of functionalized groups; thus, they are often referred to as "designer solvents". Nevertheless, in order to expand the potential applications

[a] *CICECO – Aveiro Institute of Materials, Department of Chemistry, University of Aveiro, 3810-193 Aveiro, Portugal. E-mail: maragfreire@ua.pt; Fax: +35 1234370084; Tel: +35 1234370200*
[b] *Center of Research in Ionic Liquids, Department of Chemical Engineering, Universiti Teknologi PETRONAS, Tronoh 31750, Malaysia*

† Electronic supplementary information (ESI) available: Comparison between experimental and literature solvatochromic values; correlation between experimental and predicted hydrogen-bond acidity; equation to calculate the absolute relative deviation. See DOI: 10.1039/c5cp03094c

of ILs, much more information regarding their physicochemical properties needs to be gathered. It is perhaps obvious that physicochemical properties, such as density, viscosity, surface tension and melting temperature, are essential requirements when choosing an IL for a target application. Just as important, and although less studied, is to gather information on the polarity of ILs, as this property reflects the solvation capability of these fluids. Indeed, it has previously been demonstrated that the polarity of ILs influences their solvation ability, as well as reaction rates, reaction mechanisms, product yields, enzymatic activity, among others.[10,11]

One of the methods often employed to estimate the polarity of solvents is based on the analysis of the UV-Vis spectral band shifts of solvatochromic probes, in which the position of the maximum absorption wavelength is an indication of the solvent properties. In this regard, several dyes have been used to determine the polarity of solvents, including ILs. To this end, the Dimroth–Reichardt $E_T(30)$ scale based on the dye 2,6-diphenyl-4-(2,4,6-triphenyl-1-pyridino)phenolate is usually employed.[12] However, while one-parameter $E_T(30)$ polarity scales can provide qualitative trends, they often cannot be used to correlate with other properties, such as reaction rates.[13] On the other hand, Kamlet–Taft (KT) parameters are able to describe the polarity of a given fluid into more specific characteristics, such as hydrogen-bond donating ability (α), hydrogen-bond accepting ability (β), and dipolarity/polarizability (π^*).[12] Together, and through Linear Solvation Energy Relationships (LSER), these three parameters were already shown to be able to lead to predictions on reaction rate constants, equilibrium constants, solubilities, and spectral frequencies, and based on data acquired with only a few solvents.[14] Although the LSER-KT association was initially developed for molecular organic solvents, it can also be applied to ILs.[15–17] For instance, Bini *et al.*[15] demonstrated that the hydrogen-bonding donor ability of ILs (acting as solvents) rules the Diels–Alder reactions of acrolein and methylacrylate, where the solvent effects on these reactions were examined using multi-parameter linear solvation energy relationships. Moreover, LSER-KT relationships revealed that the IL dipolarity/polarizability has a significant impact on the propagation rate coefficients in methyl methacrylate radical polymerizations.[16,17] If ILs are being studied as major solvents to replace VOCs, and for the most diverse applications, then it is necessary to analyse the contribution of each KT solvatochromic parameter to model chemical processes that yield the same or similar effects. A simplified LSER is given by the following equation:

$$XYZ = (XYZ)_0 + s(\pi^* + d\delta) + a\alpha + b\beta \quad (1)$$

where XYZ is the result of a particular solvent-dependent process, $(XYZ)_0$ is the value for the reference system, and the parameters a, b, d, and s represent solvent-independent coefficients. δ is the polarizability correction term which is equal to 0.0 for non-chlorinated solvents, 0.5 for polychlorinated solvents, and 1.0 for aromatic solvents.[14]

Although all these parameters were originally developed to describe conventional solvents, several research groups have determined these parameters for ILs to be able to compare their properties and behaviour with those of conventional solvents.[18,19] It should, however, be highlighted that the measurement of these parameters relies on the successful application of solvatochromic probes and their behaviour in ILs, which in some cases is limited by solubility and stability restrictions.[13] Furthermore, the study of the IL polarity *via* solvatochromic parameters is much more complex than in common organic solvents. While simple molecular solvents are frequently limited in the types of possible interactions with the dissolved solutes (in this case, the solvatochromic dye), ILs, due to their chemical structure and diversity, are capable of multiple types of interactions. This scenario becomes even more intricate as both the cation and the anion can have their own distinct interactions with the solute.[20,21] Therefore, because of the complexity on specific interactions between the ILs ions and the solvatochromic probes, the prediction of a polarity scale for ILs is still a major challenge.[22] This situation is even more problematic since different dyes and experimental approaches result in significantly different values of solvatochromic parameters for the same ILs.[13,15,23–40] For instance, the reported α value for the well-characterized IL 1-butyl-3-methylimidazolium bis(trifluoromethylsulfonyl)imide ($[C_4C_1im][NTf_2]$) varies from 0.51 to 0.86 (*cf.* Fig. S1 in the ESI†). For this reason, one must understand which types of interactions are reflected by a given solvent polarity scale and critically evaluate these values when making direct comparisons between scales.

Aiming at overcoming the difficulties encountered with solvatochromic probes and at the establishment of a general and well-defined polarity scale for ILs, several attempts have been made in the past few years. Monte Carlo simulations of the solvatochromic dye 2,6-diphenyl-4-(2,4,6-triphenyl-1-pyridino)-phenolate in a series of organic solvents were performed to explore the ever-popular $E_T(30)$ solvent scale.[41] Later, Znamenskiy and Kobrak employed molecular dynamics simulations to describe the solute–solvent interactions for the same probe and 1-butyl-3-methylimidazolium hexafluorophosphate, ($[C_4C_1im][PF_6]$).[20] Recently, Hunt and co-workers proposed the use of different computational descriptors for predicting α and β parameters in ILs.[42] Contreras and co-workers proposed Lewis Molecular Acidity of ionic liquids from empirical energy-density models.[43] Albeit all the results are promising, these approaches require a high computational cost and more expertise knowledge, and thus, are not suitable for routine screening. Finding simple computational tools to predict α, β, and π^* of an IL, based on their individual constituent ions, would be thus of high relevance.

Recently, Cláudio *et al.*[44] used the data available for experimental solvatochromic parameters and correlated them with hydrogen-bonding energies between different IL cation–anion pairs, estimated using the Conductor-like Screening Model for Real Solvents (COSMO-RS),[45,46] while proposing a new and extended hydrogen-bond basicity scale for ILs. Although our previous efforts represent a major advance for the characterization of the ability of IL anions to accept protons,[44] an extended hydrogen-bond acidity scale is still missing to characterize the ''overall'' polarity of ILs. Thus, in this work, we propose a

three-parameter correlation able to predict the hydrogen-bond acidity of ILs.

Due to some inconsistencies in the literature regarding the KT solvatochromic parameters for ILs, we firstly attempted their experimental determination for a wide range of bis(trifluoromethylsulfonyl)imide-based ILs (henceforth abbreviated as $[NTf_2]$-based ILs), and properly compared our data with those previously reported in the literature.[13,15,17,22–40,47–51] It should be highlighted that the hydrogen-bond acceptor strength of an IL is dominated by its anion while the hydrogen-bond donor ability is essentially controlled by the cation and only slightly depends upon the anion of the IL.[18,19] Thus, and since we were focused on developing an extended series for the hydrogen-bond acidity of ILs, ILs comprising a fixed anion ($[NTf_2]^-$) and a wide range of cations (imidazolium-, pyridinium-, piperidinium-, pyrrolidinium-, ammonium-, sulfonium-, and phosphonium-based) were selected. The $[NTf_2]$-based ILs were also chosen because most of them are liquid at room temperature, thus allowing the study of a broad range of IL cations and their impact on the IL hydrogen-bond acidity. The measured experimental data are presented and discussed in detail. This experimental section is then followed by the development of a correlation between the experimental α values with quantum chemical derived parameters, namely by three interaction energies in cation–anion pairs, estimated using COSMO-RS. Based on the results obtained, a three-parameter correlation is here proposed, aiming at predicting the hydrogen-bond acidity of a broad range of new or not yet synthesized ILs.

2. Methodology

2.1 Chemicals

The KT solvatochromic parameters were determined for the $[NTf_2]$-based ILs comprising the following cations: 1,3-dimethylimidazolium, $[C_1C_1im][NTf_2]$; 1,3-dipentylimidazolium, $[C_5C_5im][NTf_2]$; 1,3-dihexylimidazolium, $[C_6C_6im][NTf_2]$; 1,3-diheptylimidazolium, $[C_7C_7im][NTf_2]$; 1-methyl-3-propylimidazolium, $[C_3C_1im][NTf_2]$; 1-butyl-3-methylimidazolium, $[C_4C_1im][NTf_2]$; 1-methyl-3-pentylimidazolium, $[C_5C_1im][NTf_2]$; 1-hexyl-3-methylimidazolium, $[C_6C_1im][NTf_2]$; 1-heptyl-3-methylimidazolium, $[C_7C_1im][NTf_2]$; 1-methyl-3-octylimidazolium, $[C_8C_1im][NTf_2]$; 1-methyl-3-nonylimidazolium, $[C_9C_1im][NTf_2]$; 3-methyl-1-propylpyridinium, $[C_3\text{-}3\text{-}C_1py][NTf_2]$; 1-butyl-1-methylpiperidinium, $[C_4C_1pip][NTf_2]$; 1-butyl-1-methylpyrrolidinium, $[C_4C_1pyrr][NTf_2]$: butyltrimethylammonium, $[N_{4111}][NTf_2]$; triethylsulfonium, $[S_{222}][NTf_2]$; and trihexyltetradecylphosphonium, $[P_{666,14}][NTf_2]$. $[P_{666,14}][NTf_2]$ was kindly provided by Cytec Ind., while all the remaining ILs were acquired from IoLiTec (IL Technologies, Germany). In order to remove traces of water and volatile compounds, individual samples of each IL were dried at a moderate temperature (*ca.* 323 K) and at high vacuum (*ca.* 10^{-3} Pa), under constant stirring, and for a minimum period of 48 h, prior to the KT measurements. A preceding washing step with water was applied to $[P_{666,14}][NTf_2]$ and as previously reported.[52] The purities of all ILs were further checked by ^1H, ^{13}C, and ^{19}F NMR and were shown to be higher than 98 wt%.

The dyes 2,6-diphenyl-4-(2,4,6-triphenyl-*N*-pyridino)phenolate (Reichardt's dye 30) and 4-nitroaniline were purchased from Aldrich, whereas *N*,*N*-diethyl-4-nitroaniline was purchased from Alfa Aesar. The dyes were used without further purification.

2.2 Solvatochromic measurements

Individual stock solutions of the Reichardt dye, *N*,*N*-diethyl-4-nitroaniline and 4-nitroaniline, were prepared in dichloromethane. To prepare a given dye/IL solution, an appropriate volume of the dye stock solution was added to *ca.* 0.5 mL of pure IL. Residual dichloromethane was then removed under vacuum at 298 K (for 3 h). The dye/IL solution was analysed by the corresponding UV-Vis spectrum of all samples, recorded at 298 K (thermostatted sample holder) using a PC-controlled SHIMADZU UV-1700 PharmaSpec Spectrophotometer. The β parameter is determined based on the maximum wavelength, λ_{max}, of *N*,*N*-diethyl-4-nitroaniline and 4-nitroaniline, whereas α and π^* are determined with the Reichardt dye and *N*,*N*-diethyl-4-nitroaniline, respectively. Further details on the experimental procedure can be found elsewhere.[18,44]

2.3 COSMO-RS

Klamt and co-workers[45,46] developed a quantum chemical approach, known as Conductor-like Screening Model for Real Solvents (COSMO-RS), for the prediction of the thermodynamic properties of pure and mixed fluids using only the chemical structure information of the respective molecules. In COSMO-RS, molecules are treated as a collection of surface segments. An expression for the chemical potential of segments in the condensed phase is derived, and in which the interaction energies between segments are calculated from COSMO-RS. The chemical potential of each molecule is then obtained by summing the contributions of the segments. Several authors have correlated the polarity of ILs with quantum chemical parameters generated using COSMO-RS and confirmed its high capability as a correlation tool.[44,53,54]

The standard process of COSMO-RS calculations employed in this work consists of two major steps. First, the continuum solvation COSMO calculations of electronic density and molecular geometry of isolated IL cations and anions were performed with the TURBOMOLE 6.1 program package on the density functional theory (DFT) level, applying the BP functional B88-P86 with a triple-ζ valence polarized basis set (TZVP) and the resolution of identity standard (RI) approximation.[55] All the optimized structures were confirmed to be minima on the potential energy surface *via* vibrational frequency analysis. The absence of imaginary or negative frequencies indicated that the structure is a global minimum.[56] After optimization, a cosmo file containing the ideal screening charges on the molecular surface was generated and was then used in the second step – the estimation of the IL cation–anion interaction energies with the COSMO*thermX* program using the parameter file BP_TZVP_C20_0111 (COSMOlogic GmbH & Co KG, Leverkusen, Germany).[57] In COSMO-RS, the total IL cation–anion interaction

energy (E_{INT}) arises from summing the three specific interactions, namely the electrostatic-misfit (E_{MF}), hydrogen-bonding (E_{HB}), and van der Waals forces (E_{vdW}) that can be expressed as

$$E_{INT} = E_{MF} + E_{HB} + E_{vdW} \quad (2)$$

It should be highlighted that in both types of calculations, the ILs were always treated as isolated ions at the quantum chemical level. Moreover, in a previous work,[44] the best predictions of the experimental data were obtained with the lowest energy conformations or with the global minimum for both cations and anions. Thus, in this work, the lowest energy conformations of all the species involved were used in the COSMO-RS calculations.

3. Results and discussion

3.1 Experimental Kamlet–Taft solvatochromic parameters

The KT solvatochromic parameters, namely α, β, and π^*, for the $[NTf_2]$-based ILs measured in this work are reported in Table 1. Comparisons between the data determined in this work and literature data are depicted in Fig. S1–S15 in the ESI.† Most data available in the literature correspond to asymmetric 1-methyl-3-alkylimidazolium-based ILs, whereas, to the best of our knowledge, no reports for symmetric 1,3-dialkylimidazolium-based ILs are available. As depicted in Fig. S1 in the ESI,† the α values of 1-methyl-3-alkylimidazolium-based ILs obtained in this work are in close agreement with those reported by Fredlake and co-workers[40] and Mellein and co-workers,[38] and are lower than those reported by Spange and co-workers.[13,23,34] However, and in general, a closer inspection of Fig. S1 in the ESI† clearly evidences high discrepancies on the reported α values between various researchers, this being an indication on the need for developing a generalized and coherent polarity scale. These differences might be attributed to the different solvatochromic probes used and the IL purity sample and/or water content. In fact, Ab Rani and co-workers[18] have demonstrated that the presence of small amounts of impurities or water has a strong impact on the solvatochromic values. For instance, the lower values of α here obtained, when compared to those reported by Spange's group,[13,23,34] can be rationalized based on the different sets of probes used; while KT probes are here employed, these researchers utilized Catalán' probes.[13,23,34] Significant differences between β and π^* solvatochromic parameters are also observed between different authors (*cf.* Fig. S2 and S3 in the ESI,† respectively) and might also be explained by the factors previously mentioned. It should however be pointed out that the solvatochromic parameters α (1.33) and π^* (1.84) for $[C_2C_1im][NTf_2]$ reported by Fujita and co-workers,[29] for $[C_8C_1pyrr][NTf_2]$ (α = 1.00) reported by Lee and Prausnitz,[48] for $[C_4C_1pip][NTf_2]$ (α = 0.93) reported by Rai and Pandey,[24] and for $[N_{4111}][NTf_2]$ (α = 1.273) reported by Moita and co-workers[51] clearly deviate from the remaining data (*cf.* Fig. S4 to S15 in the ESI†).

Table 1 Kamlet–Taft parameters of $[NTf_2]$-based ILs using the following set of dyes: Reichardt's dye, *N*,*N*-diethyl-4-nitroaniline and 4-nitroaniline

Ionic liquids	α	β	π^*
$[C_1C_1im][NTf_2]$	0.820	0.203	0.967
$[C_3C_1im][NTf_2]$	0.779	0.231	0.955
$[C_4C_1im][NTf_2]$	0.691	0.265	0.942
$[C_5C_1im][NTf_2]$	0.640	0.260	0.950
$[C_6C_1im][NTf_2]$	0.643	0.265	0.951
$[C_7C_1im][NTf_2]$	0.649	0.282	0.942
$[C_8C_1im][NTf_2]$	0.639	0.276	0.942
$[C_9C_1im][NTf_2]$	0.634	0.265	0.942
$[C_5C_5im][NTf_2]$	0.556	0.317	0.935
$[C_6C_6im][NTf_2]$	0.562	0.326	0.926
$[C_7C_7im][NTf_2]$	0.565	0.323	0.933
$[C_3\text{-}3\text{-}C_1py][NTf_2]$	0.509	0.256	0.977
$[C_4C_1pyrr][NTf_2]$	0.469	0.284	0.940
$[C_4C_1pip][NTf_2]$	0.444	0.255	0.940
$[S_{222}][NTf_2]$	0.514	0.181	0.946
$[N_{4111}][NTf_2]$	0.583	0.273	0.914
$[P_{666,14}][NTf_2]$	0.235	0.457	0.860

In general, and from the data provided in Table 1, the α values of the studied $[NTf_2]$-based ILs vary significantly from 0.235 (for $[P_{666,14}][NTf_2]$) to 0.820 (for $[C_1C_1im][NTf_2]$), while the β and π^* values are less divergent. This wide-range of variation in the α value clearly supports the well-known primary cation dependence of the hydrogen-bond acidity of ILs, in agreement with literature data.[18,19] While β and π^* values do not significantly vary among the various compounds studied, there is still a small, but nonetheless clear, dependence on the IL cation. For instance, the β values vary between 0.181 (for $[S_{222}][NTf_2]$) and 0.457 (for $[P_{666,14}][NTf_2]$) – *cf.* Table 1 – suggesting that the IL cation can be also used to fine-tune the basicity of the ILs (dominated by the anion). In the same line, the π^* values (a measure of non-specific interactions such as polarizability, dipole–dipole interactions, and dipole-induced dipole interactions) vary from 0.860 to 0.977. These overall results further stress that the IL cation, to some extent, can be used to tune the hydrogen-bond basicity and dipolarity/polarizability of ILs.

Since all the studied ILs share the same $[NTf_2]^-$ anion, their solvatochromic parameters are a result of the cation head group, the number of aliphatic tails and their alkyl side chain length. Fig. 1 depicts the α values as a function of the total number of carbons at the aliphatic moieties of the cation, *N*. Concerning the cation head group, it is clear that ILs bearing the imidazolium cation present higher α values than piperidinium-, pyridinium-, pyrrolidinium-, tetraalkylammonium-, tetraalkylphosphonium- and sulfonium-based ILs. The high acidity of imidazolium-based ILs is mainly a result of the acidic hydrogen attached to the carbon between the two nitrogen atoms in the ring. Next to imidazolium-based ILs in terms of acidity is, surprisingly, $[N_{4111}][NTf_2]$, followed by $[S_{222}][NTf_2]$, $[C_3\text{-}3\text{-}C_1py][NTf_2]$, $[C_4C_1pyrr][NTf_2]$, $[C_4C_1pip][NTf_2]$, and $[P_{666,14}][NTf_2]$ (which has the lowest acidity). It appears that, for the cyclic cations, the ILs with aromatic rings possess higher acidity when compared with the corresponding non-aromatic rings. Also, ILs comprising 5-member rings display a higher ability to donate protons than the 6-member ones (both for saturated or aromatic cations). Thus, the acidity of cyclic ILs derives mainly from the cation aromaticity and also from the number of atoms forming the ring. This higher acidity provided by aromatic and 5-member ring cations correlates well with their ability to be solvated by water by enhanced hydrogen-bonding, either in binary[58] or

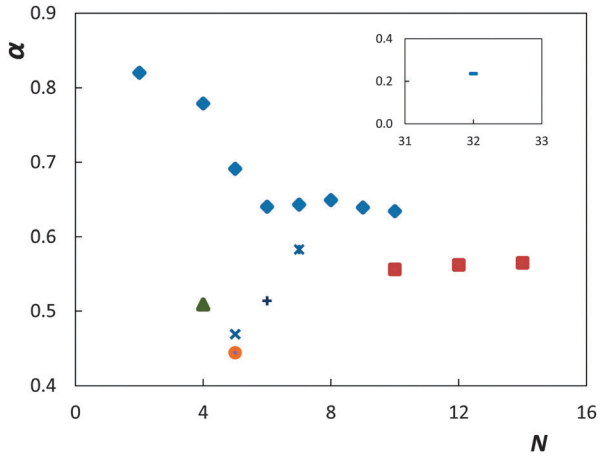

Fig. 1 Experimental hydrogen-bond acidity, α, of [NTf_2]-based ILs as a function of the total number of carbon atoms at the alkyl chains, *N*. Symbols: (♦), 1-methyl-3-alkylimidazolium-based asymmetric ILs; (■), 1,3-dialkylimidazolium-based symmetric ILs; (▲), [C_3-3-C_1py][NTf_2]; (●), [C_4C_1pip][NTf_2]; (×), [C_4C_1pyrr][NTf_2]; (+), [S_{222}][NTf_2]; (*), [N_{4111}][NTf_2]; and (—), [$P_{666,14}$][NTf_2].

ternary aqueous systems.[59] On the other hand, for the non-cyclic ILs ([N_{4111}][NTf_2], [S_{222}][NTf_2] and [$P_{666,14}$][NTf_2]) it is very interesting to point out that, even though [N_{4111}][NTf_2] contains a higher total number of carbons at the alkyl chains (N = 7), it presents a similar acidity when compared to the aromatic and symmetric 1,3-dialkylimidazolium-based ILs, and even higher than other ILs with a lower N value, *e.g.* [S_{222}][NTf_2] (N = 6). This distinct behaviour might be attributed to the charge distribution/contribution of the cation core and its adjacent methylene groups. By Natural Population Analysis,[60] it was shown that the alpha hydrogens, H_α, the hydrogens of the methylene group (–CH_3) directly connected to N of $[N_{4111}]^+$, are more positive than in the case of H_α of –CH_2 connected to S in $[S_{222}]^+$. Consequently, [N_{4111}][NTf_2] displays a higher acidity when compared with [S_{222}][NTf_2], as experimentally observed. In this context, the charge distribution/contribution of the cation also plays a major role in the acidity of a given IL. This charge distribution also has a significant impact on other properties, such as in the phase diagrams of binary IL-water systems, densities and viscosities, as previously shown.[60,61] On the other hand, the C–H bonds of the alkyl groups in tetraalkylphosphonium ILs are hardly polarised compared to tetraalkylammonium, which is clearly shown by the low α-value of the former IL. This behaviour can be attributed to the different charge distribution/contribution of the ammonium- and phosphonium-based IL cations as previously demonstrated by Carvalho *et al.*[60,61] The higher acidity afforded by ammonium-based ILs also correlates well with their lower ability to form two-aqueous phase systems reflected by a higher ability to hydrogen-bond with water.[62]

Two sets of imidazolium-based ILs were also studied: one with 1-methyl-3-alkylimidazolium-based asymmetric ILs and the other consisting of 1,3-dialkylimidazolium-based symmetric ILs. These two sets allow the study of the impact of the cation symmetry on the IL acidity. In general, the α values of asymmetric ILs are higher than for the respective symmetric isomers (*e.g.*, [C_9C_1im][NTf_2] (α = 0.634) *vs.* [C_5C_5im][NTf_2] (α = 0.556)). This behaviour can be explained by the partial positive charge distribution of the cation head group and accessibility;[63] two longer alkyl chains at symmetric ILs produce a sterical shielding of the cationic centre, leading thus to a more difficult "access" of the solvatochromic dye to establish hydrogen bonds with the IL cation. This trend agrees well with the higher ability of symmetric ILs to solubilize water compared to that displayed by the asymmetric series of ILs.[63–64] Moreover, with the set of ILs studied, it is also possible to study the origin of the IL acidity derived from the aliphatic moieties. First, for both symmetric and asymmetric imidazolium-based ILs, the hydrogen-bond acidity decreases with the increase in the number of carbon atoms at the alkyl chains, in agreement with the literature.[13,34,37] The same is valid for other ILs with different cation cores, such as monosubstituted pyridinium-,[13,23] disubstituted pyridinium-,[38] pyrrolidinium,[32] piperidinium-,[50] and sulfonium-based[13] ILs. Furthermore, it is also interesting to highlight that the acidity of asymmetric ILs significantly decreases with increasing alkyl chain length from [C_1C_1im][NTf_2] to [C_5C_1im][NTf_2], while presenting similar values between [C_5C_1im][NTf_2] and [C_9C_1im][NTf_2]. There seems to be a trend shift in the acidity of asymmetric imidazolium-based ILs as a function of alkyl chain length, to the best of our knowledge, here reported for the first time. These changes in the monotonic behaviour along the alkyl side chain length are related to the nanostructural organization of the liquid above a critical alkyl chain length (CAL) as originally proposed by Canongia Lopes and Pádua[65] using molecular dynamics simulations. Moreover, this macroscopic segregation behaviour has been shown to be a major feature in the ionic liquid bulk phase and as reflected in the thermophysical properties of ILs.[66–73] Similar trend shifts were observed in the IL viscosity,[66–67] surface tension,[68] vapour pressure,[69,70] heat capacity,[71] among others.[72,73]

It is, however, thought-provoking to highlight that different trends on the IL acidity with increasing alkyl chain length have also been reported.[48,49] Lee and Prausnitz[48] reported that the hydrogen-bond acidity of pyrrolidinium-based ILs decreases with increasing the alkyl side chain length from [C_3C_1pyrr][NTf_2] (α = 0.74) to [C_4C_1pyrr][NTf_2] (α = 0.52); however, the α value increases for [C_8C_1pyrr][NTf_2] (α = 1.00), almost twice than that for [C_4C_1pyrr][NTf_2]. Khupse and Kumar[49] also reported the increase of the α value with the increase of the alkyl side chain length of pyrrolidinium-based ILs, from [C_4C_1pyrr][NTf_2] to [C_6C_1pyrr][NTf_2]. Nevertheless, with the lack of data for pyrrolidinium-based ILs, it is tricky to evaluate whether this peculiarity is indeed due to a distinct behaviour of pyridinium-based ILs with long alkyl side chain lengths. More experimental data for solvatochromic parameters of pyrrolidinium-based ILs with different alkyl side chain lengths are required to understand the phenomena behind this observation.

Overall, and based on the results here measured, combined with those reported in the literature (and shown in ESI†), it is evident that there is a great deal of inconsistency regarding the establishment of a polarity scale for ILs. This factor is a major obstacle when an appropriate IL has to be selected for a

specific application. Therefore, and based on the new experimental data provided, we attempted at developing a correlation for the ability of the IL cation to establish hydrogen-bonds so that an appropriate IL can be chosen for a specific application without extensive and time-consuming experiments – results shown below.

3.2 Estimation of the hydrogen-bond acidity of ILs

Taking into account all the difficulties found in measuring the solvatochromic parameters of ILs, and the discrepancy of the reported values between authors, reliable estimation methods for such a property are desirable, especially if they can provide not only a quantitative classification but an extended scale that can be used to understand their behaviour in the most diverse situations. While some simpler ILs can nowadays be reasonably well described by molecular modelling, the description of the IL-dye interactions still is a challenge for such simulation approaches, resulting in high computational costs and expert knowledge is required. Therefore, nowadays, molecular modelling is still not a suitable method for routine screening.[42] On the other hand, COSMO-RS, originally developed by Klamt and co-workers,[45,46] is regarded as a valuable method to predict the thermodynamic properties of ILs and their mixtures based on the unimolecular quantum chemical calculations for the individual species. In particular for ILs, it only requires the molecular structure of their ions in order to generate a given parameter required to correlate with the experimental values. In this context, we used four quantum chemical parameters generated using COSMO-RS, namely electrostatic-misfit (E_{MF}), hydrogen-bond (E_{HB}), and van der Waals (E_{vdW}) energies, as well as the sum of these energies (E_{INT}) of IL cation–anion pairs (with no solvent involved). Cláudio and co-workers[44] have successfully correlated the β values of ILs with the E_{HB} descriptor obtained from COSMO-RS, and provided an extended scale for the hydrogen-bond basicity of ILs. In this work, we applied a similar procedure aiming at developing a correlation between the experimental α values and the COSMO-RS parameters so that an extended scale able to characterize the hydrogen-bond acidity of ILs could be provided.

As a preliminary step, we attempted the correlation between the experimental IL hydrogen-bond acidity values and the different COSMO-RS descriptors, resulting on the equations shown in Table 2. The accuracy of the correlation to describe each training set of α values can be accessed by the respective correlation coefficients (R^2), which can be mathematically interpreted as the balanced reduction of the total variation associated with the independent variable, and the absolute average relative deviation (AARD), which measures the difference between the real/experimental and predicted values. Further details can be found in the ESI.† The correlations using only one COSMO-RS parameter are described by eqn (3)–(6) in Table 2, along with their statistical parameters. As shown, one-parameter correlations using only E_{INT}, E_{MF} or E_{vdW} are not statistically relevant, a clear indication that the hydrogen-bond acidity of IL cations is not governed by electrostatic and van der Waals interactions. On the other hand, and as expected, the experimental α values are adequately correlated with E_{HB}, with R^2 and AARD values of 0.8768 and 7.6%, respectively – *cf.* eqn (5) in Table 2. Accordingly, for the one-parameter models, Fig. S16–19 in the ESI† demonstrate that there is a close agreement between the experimental *versus* predicted α values using E_{HB}, while the same could not be observed when using the other three isolated energies. This trend evidences that the hydrogen-bonding energy between the cation–anion pairs plays a significant role in the acidity of ILs and their ability to establish hydrogen bonds with the most diverse species and/or solvents.

It is important to note that eqn (5) is based on the same type of descriptors used in our previous work, E_{HB}.[44] This is to be expected, since the hydrogen bond strength between IL cation–anion pairs is the most significant type of energy describing their ability to act as hydrogen bond donors and acceptors. Even so, a higher correlation coefficient was obtained for the description of the hydrogen-bond acceptor ability of ILs ($\beta - E_{HB}$), dominated by the IL anion ($R^2 = 0.9234$).[44] It seems thus that while the hydrogen-bond basicity of ILs depends almost exclusively on the strength of the anion to act as a hydrogen-bond acceptor, the lower R^2 (0.8768) obtained in this work for the description of the hydrogen-bond acidity of ILs highlights that the IL acidity cannot be solely described by the ability of the IL cation to donate protons, and that other types of interactions also contribute to the general IL acidity. To improve the obtained correlation and to infer on the existence of other types of interactions influencing the acidity of a target IL, we then attempted multi-parameter correlations by combining two or three cation–anion interaction energies. In the two-parameters model, the combination of E_{HB} with either E_{MF} or E_{vdW} (*cf.* eqn (7) and (8) in Table 2) improves the correlation coefficient; on the other hand, the combination of E_{MF} and E_{vdW} (*cf.* eqn (9) in Table 2) decreases the correlation coefficient to even lower values than those obtained with the single E_{HB}

Table 2 Correlations between the experimental hydrogen-bond acidity (α) of ILs and the cation–anion interaction energies estimated using COSMO-RS. The respective correlation coefficient, R^2, and absolute average relative deviation, AARD, are also provided

	R^2	AARD/%	Equation
$\alpha = ((0.0041 \pm 0.0016) \times E_{INT}) + (0.7703 \pm 0.0779)$	0.3295	17.6	(3)
$\alpha = ((-0.0191 \pm 0.0058) \times E_{MF}) + (1.2783 \pm 0.2122)$	0.4394	17.8	(4)
$\alpha = ((-0.0539 \pm 0.0054) \times E_{HB}) + (0.1789 \pm 0.0422)$	0.8768	7.6	(5)
$\alpha = ((0.0036 \pm 0.0011) \times E_{vdW}) + (0.8617 \pm 0.0897)$	0.4346	16.1	(6)
$\alpha = ((-0.0081 \pm 0.0023) \times E_{MF}) + ((-0.0462 \pm 0.0045) \times E_{HB}) + (0.5309 \pm 0.1040)$	0.9374	4.4	(7)
$\alpha = ((-0.0467 \pm 0.0052) \times E_{HB}) + ((0.0013 \pm 0.0005) \times E_{vdW}) + (0.3362 \pm 0.0685)$	0.9206	4.8	(8)
$\alpha = ((-0.0111 \pm 0.0221) \times E_{MF}) + ((0.0015 \pm 0.0042) \times E_{vdW}) + (1.1087 \pm 0.4989)$	0.4455	16.9	(9)
$\alpha = ((-0.0164 \pm 0.0073) \times E_{MF}) + ((-0.0474 \pm 0.0046) \times E_{HB}) + ((-0.0017 \pm 0.0014) \times E_{vdW}) + (0.6934 \pm 0.1696)$	0.9441	3.9	(10)

parameter model. The respective graphical representations are given in Fig. S20–S22 in the ESI.† Overall, while hydrogen bond interactions between cation–anion pairs dominate the hydrogen-bond acidity of ILs, electrostatic-misfit and van der Waals forces also play a minor role and cannot be discarded in the development of the acidity scale of ILs. Finally, the use of a three-parameter correlation to describe the hydrogen-bond acidity of ILs leads to an improvement in the correlation coefficient, up to 0.9441 – *cf.* Table 2. The fact that eqn (7), (8), and (10) better correlate the training set data when compared to that obtained in a previous work,[44] indicates that the acidity of ILs, unlike the basicity, may depend not only on the hydrogen bond strength of the IL but also, to some extent, on electrostatic and van der Waals forces.

In summary, these results indicate that the structural factors that influence the IL hydrogen-bond acidity can be described by a fixed set of quantum-derived parameters, namely by cation–anion pairs energies. Eqn (10) was then used to estimate the α values of neat ILs. Fig. 2 depicts the relationship between the experimental and estimated α values using eqn (10) (the comparison using eqn (3)–(9) is given in Fig. S16–S21 in the ESI†). In general, there is a very close agreement between the experimental and predicted α values (AAD = 3.9%) meaning that eqn (10) can be used to predict the hydrogen-bond acidity of a wide variety of ILs, and independently of the IL cation core or the alkyl side chain length, with reasonable accuracy. For instance, among the ILs evaluated in this study, the most acidic is $[C_1C_1im][NTf_2]$, whereas that displaying the lowest α value is $[P_{666,14}][NTf_2]$ – a fact detected and well described by eqn (10). In addition, the prediction results concerning the influence of the alkyl side chain length on the hydrogen-bond donor strength of the IL cation are consistent with the experimental data, as well as with data published by other authors.[13,23,32,38,50] The variety of cations used, along with the high variability of α values (between 0.235 and 0.820), guarantees the widespread application of eqn (10), and further validates the *a priori* cation–anion interaction energy descriptors for the prediction of the hydrogen-bond donor ability of ILs.

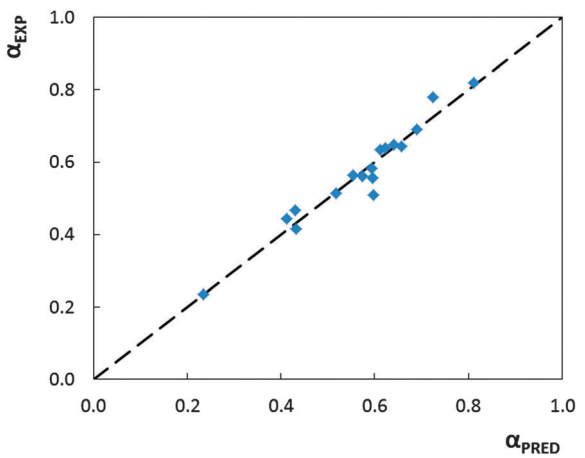

Fig. 2 Correlation between experimental (α_{EXP}) and predicted (α_{PRED}) values of hydrogen-bond acidity of $[NTf_2]$-based ILs using eqn (10). R^2 = 0.9441 and AAD = 3.9%.

3.3 Predictive values for the hydrogen-bond acidity of ILs

In the past few years, considerable progress has been made in identifying structure-related descriptors aimed at predicting the polarity of ILs.[20,41,42,53,54] Driven by the prediction results presented in Fig. 2, eqn (10) was then tested in order to assess its predictive ability towards new ILs or ILs with no experimental data yet available. A new data set comprising similar structures, none of which are present in the training data set, was built and their predicted α values are given in Table 3. Imidazolium cations bearing not only linear and saturated alkyl side chains were considered, but also containing functionalized groups (–OH and $-NH_2$), and with a different number of aliphatic moieties at the cation – first set. The other set is constituted by 1-alkyl-2,3-dimethylimidazolium-, 1,3-dialkylimidazolium-, 1-alkylpyridinium-, 1-alkyl-1-methylpyrrolidinium-, 1-alkyl-1-methylpiperidinium-, sulfonium-, phosphonium-, and ammonium-based ILs. The set extent can be as large as desired since the correlation method developed only requires cation–anion interaction energies that can be estimated using COSMO-RS. The full name and abbreviation of a large plethora of ILs, along with their cation–anion interaction energy descriptors, are given in Table 3.

To examine the predictive ability of the model proposed, the ILs listed in Table 3 can be considered as two groups. The first group consists of ILs with a few structural differences, for instance comprising the methylation of the most acidic hydrogen at 1-alkyl-3-methylimidazolium to form the 1-alkyl-2,3-dimethylimidazolium cation. $[C_4C_1C_1im][NTf_2]$ has a lower α_{pred} (due to a decrease in the hydrogen-bond interaction energies) when compared with $[C_4C_1im][NTf_2]$, and in agreement with reported experimental data by other authors.[13,23] Moreover, the incorporation of polar functionalized groups into the alkyl side chain terminal of 1-alkyl-3-methylimidazolium to form 1-hydroxyalkyl-3-methylimidazolium, as in the case of $[C_2C_1im][NTf_2]$ to give $[HO\text{-}C_2C_1im][NTf_2]$, increases the hydrogen-bond interaction energy and, consequently, increases α_{PRED}, while agreeing with the experimental trend.[33,74] These results are notable while supporting the capacity of the developed equation to describe the hydrogen-bond acidity of ILs since these evidences were found based on a correlation developed with ILs with different chemical structures and not having functionalized groups or more than two aliphatic tails at the imidazolium cation.

For the second group of ILs, the predicted α values decrease with increasing alkyl side chain length, regardless of the cation core, and in agreement with the literature.[13,23,32,38,50] Furthermore, for the cyclic-based ILs with the same number of carbon atoms in the alkyl chains, the predicted α values follow the expected trend: 1-alkyl-3-methylimidazolium > 1,3-dialkylimidazolium ~ 1-alkylpyridinium > 1-alkyl-1-methylpyrrolidinium > 1-alkyl-1-methylpiperidinium. For the non-cyclic cations, ammonium-based ILs are more acidic than the phosphonium-based fluids. In summary, and based on these overall trends, the proposed correlation allows the prediction of

Table 3 Predicted hydrogen-bond acidity (α_{PRED}) values of [NTf_2]-based ILs. The cation list is presented based on the head group and in a decreasing order of hydrogen-bond acidity of the IL cation

Cation	Abbreviation	E_{INT}	E_{MF}	E_{HB}	E_{vdW}	α_{PRED}
1-Alkyl-3-methylimidazolium						
1,3-Dimethylimidazolium	$[C_1C_1im]^+$	−34.405	29.269	−10.612	−54.321	0.813
1-Ethyl-3-methylimidazolium	$[C_2C_1im]^+$	−34.083	30.924	−9.771	−57.538	0.750
1-Methyl-3-propylimidazolium	$[C_3C_1im]^+$	−36.090	32.325	−9.642	−60.988	0.727
1-Butyl-3-methylimidazolium	$[C_4C_1im]^+$	−37.985	33.774	−9.279	−65.077	0.692
1-Methyl-3-pentylimidazolium	$[C_5C_1im]^+$	−40.561	34.913	−9.224	−68.777	0.677
1-Hexyl-3-methylimidazolium	$[C_6C_1im]^+$	−43.162	36.017	−9.068	−72.649	0.659
1-Heptyl-3-methylimidazolium	$[C_7C_1im]^+$	−45.936	37.056	−8.958	−76.543	0.643
1-Methyl-3-octylimidazolium	$[C_8C_1im]^+$	−49.070	38.084	−8.768	−80.597	0.624
1-Methyl-3-nonylimidazolium	$[C_9C_1im]^+$	−51.630	38.954	−8.725	−84.397	0.615
1-Decyl-3-methylimidazolium	$[C_{10}C_1im]^+$	−54.859	39.885	−8.451	−88.512	0.593
1,3-Dimethylimidazolium						
1,3-Diethylimidazolium	$[C_2C_2im]^+$	−35.796	32.413	−9.334	−60.896	0.710
1,3-Dipropylimidazolium	$[C_3C_3im]^+$	−39.456	34.826	−8.893	−68.159	0.662
1,3-Dibutylimidazolium	$[C_4C_4im]^+$	−45.332	36.836	−8.664	−75.831	0.631
1,3-Dipentylimidazolium	$[C_5C_5im]^+$	−50.409	38.600	−8.307	−83.390	0.598
1,3-Dihexylimidazolium	$[C_6C_6im]^+$	−56.948	40.224	−8.118	−91.439	0.577
1,3-Diheptylimidazolium	$[C_7C_7im]^+$	−63.330	41.699	−7.905	−99.508	0.557
1,3-Dioctylimidazolium	$[C_8C_8im]^+$	−69.580	43.039	−7.631	−107.371	0.536
1,3-Dinonylimidazolium	$[C_9C_9im]^+$	−76.202	44.287	−7.440	−115.405	0.521
1,3-Didecylimidazolium	$[C_{10}C_{10}im]^+$	−84.732	45.459	−7.434	−124.161	0.518
1-Alkyl-2,3-dimethylimidazolium						
1,2,3-Trimethylimidazolium	$[C_1C_1C_1im]^+$	−31.164	30.896	−6.394	−57.020	0.586
1-Ethyl-2,3-dimethylimidazolium	$[C_2C_1C_1im]^+$	−31.622	32.434	−5.919	−60.147	0.543
1,2-Methyl-3-propylimidazolium	$[C_3C_1C_1im]^+$	−33.699	33.797	−5.766	−63.740	0.519
1-Butyl-2,3-methylimidazolium	$[C_4C_1C_1im]^+$	−36.148	35.115	−5.464	−67.705	0.490
1,2-Methyl-3-pentylimidazolium	$[C_5C_1C_1im]^+$	−39.506	36.191	−5.621	−71.475	0.486
1-Hexyl-2,3-methylimidazolium	$[C_6C_1C_1im]^+$	−41.474	37.241	−5.309	−75.297	0.461
1-Hydroxyalkyl-3-methylimidazolium						
1-Hydroxymethyl-3-methylimidazolium	$[HO\text{-}C_1C_1im]^+$	−57.393	29.403	−33.475	−54.740	1.920
1-(2-Hydroxyethyl)-3-methylimidazolium	$[HO\text{-}C_2C_1im]^+$	−55.805	30.405	−29.257	−58.093	1.705
1-(3-Hydroxypropyl)-3-methylimidazolium	$[HO\text{-}C_3C_1im]^+$	−55.186	32.731	−27.644	−61.974	1.595
1-(4-Hydroxybutyl)-3-methylimidazolium	$[HO\text{-}C_4C_1im]^+$	−56.779	34.741	−27.348	−65.931	1.554
1-(5-Hydroxypentyl)-3-methylimidazolium	$[HO\text{-}C_5C_1im]^+$	−58.745	36.294	−27.123	−69.677	1.524
1-(6-Hydroxyhexyl)-3-methylimidazolium	$[HO\text{-}C_6C_1im]^+$	−60.973	37.663	−26.908	−73.499	1.498
1-(7-Hydroxyheptyl)-3-methylimidazolium	$[HO\text{-}C_7C_1im]^+$	−63.877	38.836	−26.834	−77.400	1.482
1-(8-Hydroxyoctyl)-3-methylimidazolium	$[HO\text{-}C_8C_1im]^+$	−66.388	39.990	−26.547	−81.410	1.456
1-(9-Hydroxynonyl)-3-methylimidazolium	$[HO\text{-}C_9C_1im]^+$	−68.892	40.965	−26.463	−85.181	1.442
1-(10-Hydroxydecyl)-3-methylimidazolium	$[HO\text{-}C_{10}C_1im]^+$	−71.780	42.006	−26.134	−89.319	1.417
1-Aminoalkyl-3-methylimidazolium						
1-Aminomethyl-3-methylimidazolium	$[H_2N\text{-}C_1C_1im]^+$	−45.021	29.621	−18.757	−57.099	1.207
1-(2-Aminoethyl)-3-methylimidazolium	$[H_2N\text{-}C_2C_1im]^+$	−42.101	32.574	−17.501	−59.909	1.102
1-(3-Aminopropyl)-3-methylimidazolium	$[H_2N\text{-}C_3C_1im]^+$	−42.913	35.130	−17.222	−63.057	1.051
1-(4-Aminobutyl)-3-methylimidazolium	$[H_2N\text{-}C_4C_1im]^+$	−45.011	37.208	−16.845	−67.124	1.005
1-(5-Aminopentyl)-3-methylimidazolium	$[H_2N\text{-}C_5C_1im]^+$	−47.026	38.650	−16.778	−70.739	0.984
1-(6-Aminohexyl)-3-methylimidazolium	$[H_2N\text{-}C_6C_1im]^+$	−48.594	39.832	−16.440	−74.605	0.955
1-(7-Aminoheptyl)-3-methylimidazolium	$[H_2N\text{-}C_7C_1im]^+$	−52.096	41.047	−16.517	−78.458	0.946
1-(8-Aminooctyl)-3-methylimidazolium	$[H_2N\text{-}C_8C_1im]^+$	−55.010	42.134	−16.265	−82.487	0.923
1-(9-Aminononyl)-3-methylimidazolium	$[H_2N\text{-}C_9C_1im]^+$	−57.685	43.111	−16.198	−86.406	0.911
1-(10-Aminodecyl)-3-methylimidazolium	$[H_2N\text{-}C_{10}C_1im]^+$	−60.517	44.081	−15.972	−90.381	0.891
1-Alkylpyridinium						
1-Methylpyridinium	$[C_1py]^+$	−33.876	28.775	−10.524	−53.370	0.815
1-Ethylpyridinium	$[C_2py]^+$	−34.060	30.457	−9.527	−56.508	0.744
1-Propylpyridinium	$[C_3py]^+$	−35.208	31.974	−9.127	−59.978	0.706
1-Butylpyridinium	$[C_4py]^+$	−37.609	33.387	−8.932	−63.898	0.680
1-Pentylpyridinium	$[C_5py]^+$	−40.552	34.653	−8.741	−67.780	0.656
1-Hexylpyridinium	$[C_6py]^+$	−42.681	35.780	−8.574	−71.592	0.637
1-Heptyllpyridinium	$[C_7py]^+$	−45.813	36.862	−8.470	−75.534	0.621
1-Octylpyridinium	$[C_8py]^+$	−48.364	37.870	−8.274	−79.426	0.602
1-Nonylpyridinium	$[C_9py]^+$	−51.335	38.811	−8.152	−83.334	0.587
1-Decylpyridinium	$[C_{10}py]^+$	−54.207	39.718	−7.980	−87.291	0.571
1-Alkyl-1-methylpyrrolidinium						
1,3-Dimethylpyrrolidinium	$[C_1C_1pyrr]^+$	−28.601	30.381	−5.912	−54.425	0.566

Table 3 (*continued*)

Cation	Abbreviation	E_{INT}	E_{MF}	E_{HB}	E_{vdW}	α_{PRED}
1-Ethyl-1-methylpyrrolidinium	$[C_2C_1pyrr]^+$	−27.527	32.038	−4.617	−57.313	0.481
1-Methyl-1-propylpyrrolidinium	$[C_3C_1pyrr]^+$	−29.166	33.551	−4.477	−61.011	0.455
1-Butyl-1-methylpyrrolidinium	$[C_4C_1pyrr]^+$	−31.907	34.882	−4.322	−64.898	0.433
1-Methyl-1-pentylpyrrolidinium	$[C_5C_1pyrr]^+$	−34.157	36.084	−4.133	−68.822	0.411
1-Hexyl-1-methylpyrrolidinium	$[C_6C_1pyrr]^+$	−36.851	37.196	−4.021	−72.774	0.394
1-Heptyl-1-methylpyrrolidinium	$[C_7C_1pyrr]^+$	−39.779	38.218	−3.931	−76.730	0.380
1-Methyl-1-octylpyrrolidinium	$[C_8C_1pyrr]^+$	−42.683	39.178	−3.838	−80.686	0.367
1-Methyl-1-nonylpyrrolidinium	$[C_9C_1pyrr]^+$	−45.630	40.093	−3.736	−84.664	0.354
1-Decyl-1-methylpyrrolidinium	$[C_{10}C_1pyrr]^+$	−48.840	40.948	−3.715	−88.648	0.346
1-Alkyl-1-methylpiperidinium						
1,3-Dimethylpiperidinium	$[C_1C_1pip]^+$	−29.507	31.470	−5.734	−56.611	0.543
1-Ethyl-1-methylpiperidinium	$[C_2C_1pip]^+$	−28.910	33.019	−4.452	−59.544	0.460
1-Methyl-1-propylpiperidinium	$[C_3C_1pip]^+$	−31.199	34.438	−4.270	−63.310	0.435
1-Butyl-1-methylpiperidinium	$[C_4C_1pip]^+$	−33.697	35.662	−4.132	−67.218	0.415
1-Methyl-1-pentylpiperidinium	$[C_5C_1pip]^+$	−36.377	36.751	−4.027	−71.111	0.399
1-Hexyl-1-methylpiperidinium	$[C_6C_1pip]^+$	−39.266	37.770	−3.922	−75.069	0.384
1-Heptyl-1-methylpiperidinium	$[C_7C_1pip]^+$	−42.180	38.710	−3.855	−79.008	0.372
1-Methyl-1-octylpiperidinium	$[C_8C_1pip]^+$	−45.108	39.630	−3.733	−83.036	0.358
1-Methyl-1-nonylpiperidinium	$[C_9C_1pip]^+$	−48.275	40.489	−3.628	−87.011	0.346
1-Decyl-1-methylpiperidinium	$[C_{10}C_1pip]^+$	−51.278	41.293	−3.575	−91.006	0.338
Tetraalkylammonium						
Cholinium	$[Ch]^+$	−47.802	28.699	−24.425	−53.905	1.491
Tetramethylammonium	$[N_{1111}]^+$	−30.759	27.679	−9.105	−50.608	0.759
Ethyltrimethylammonium	$[N_{2111}]^+$	−30.146	29.475	−7.461	−53.483	0.655
Butyltrimethylammonium	$[N_{4111}]^+$	−32.723	32.723	−7.103	−60.740	0.596
Hexyltrimethylammonium	$[N_{6111}]^+$	−37.193	35.440	−6.559	−68.589	0.539
Ethyldimethylpropylammonium	$[N_{2113}]^+$	−31.577	32.750	−5.715	−60.016	0.527
Heptyltrimethylammonium	$[N_{7111}]^+$	−40.410	36.595	−6.554	−72.505	0.527
Trimethyloctylammonium	$[N_{1118}]^+$	−43.728	37.787	−6.238	−76.657	0.499
Butyldimethylpropylammonium	$[N_{1134}]^+$	−35.854	35.387	−5.377	−67.597	0.481
Trimethyltetradecylammonium	$[N_{111,14}]^+$	−61.549	43.200	−5.550	−100.610	0.420
Tetraethylammonium	$[N_{2222}]^+$	−29.787	33.971	−3.522	−61.674	0.403
Tributylmethylammonium	$[N_{4441}]^+$	−44.460	39.366	−3.681	−82.275	0.359
Triethylpentylammonium	$[N_{2225}]^+$	−36.669	37.300	−3.133	−73.069	0.350
Hexyltrimethylammonium	$[N_{2226}]^+$	−40.333	38.264	−3.122	−77.077	0.341
Heptyltriammonium	$[N_{2227}]^+$	−42.458	39.122	−3.004	−80.935	0.328
Tetrapropylammonium	$[N_{3333}]^+$	−39.393	38.226	−2.868	−76.244	0.327
Triethyloctylammonium	$[N_{2228}]^+$	−45.545	39.971	−2.926	−84.922	0.317
Tetrabutylammonium	$[N_{4444}]^+$	−51.975	41.379	−2.569	−92.699	0.291
Methyltrioctylammonium	$[N_{1888}]^+$	−83.725	46.991	−2.883	−130.516	0.283
Trialkylsulfonium						
Dimethylphenylsulfonium	$[S_{11Ph}]^+$	−39.837	32.204	−9.986	−63.341	0.750
Diethylmethylsulfonium	$[S_{221}]^+$	−33.419	30.526	−7.816	−58.338	0.663
Ethylmethylphenylsulfonium	$[S_{21Ph}]^+$	−38.425	33.471	−8.058	−65.883	0.640
Triethylsulfonium	$[S_{222}]^+$	−32.757	32.436	−5.375	−61.676	0.519
Tetraalkylphosphonium						
Benzyltriphenylphosphonium	$[P_{Bz(Ph)3}]^+$	−55.485	43.312	−4.754	−95.492	0.369
Triisobutylmethylphosphonium	$[P_{(i\text{-}4)3,1}]^+$	−43.459	38.871	−3.772	−80.571	0.369
Tributylmethylphosphonium	$[P_{4441}]^+$	−47.319	40.342	−2.592	−86.573	0.298
Tetrabutylphosphonium	$[P_{4444}]^+$	−53.215	41.557	−2.602	−93.860	0.292
Trimethyloctylphosphonium	$[P_{1888}]^+$	−86.482	47.263	−2.523	−132.745	0.265
Trihexyltetradecylphosphonium	$[P_{666,14}]^+$	−109.882	49.526	−1.698	−159.881	0.239

a correct qualitative trend on the ILs acidity. Such information, ultimately, is valuable for the design and applications of a target IL with pre-defined hydrogen-bond acidity and/or polarity.

The correlation here proposed is able to establish a quantitative connection between the hydrogen-bond donating strength of a given IL and the cation–anion interaction energies, estimated using COSMO-RS. In this way, the equation proposed has two-fold utility: (i) it allows the prediction of the hydrogen-bond acidity values of ILs not yet synthesized or for which no polarity data are available; and (ii) it helps in the understanding of the molecular-level mechanisms ruling the IL acidity representing thus a powerful and intuitive tool for a more rational design of ILs with desired polarity.

Table 3 lists the COSMO-RS interaction energies and predicted hydrogen-bond acidity for a plethora of IL cations – the most extended series reported to date. This extended polarity scale of the ability of the IL cation to hydrogen-bond can provide *a priori* information to select an improved IL for a

specific application before extensive and time-consuming experiments. In summary, the proposed correlation opens up the door to the creation of ILs with pre-defined hydrogen-bond acidity for target applications.

4. Conclusions

ILs have been claimed as potential replacements for VOCs in modern and sustainable ''greener'' processes of the chemical industry. In this context, the IL polarity is a crucial property required for a rational design of ILs either to define their phase behaviour and solvation ability or when directly involved in chemical reactions. Many experimental attempts have been carried out to define the IL polarity; however, there are several inconsistencies on the reported values. Albeit some theoretical/computational approaches have been attempted to overcome the experimental limitations, these techniques require advanced knowledge and ''expensive'' computational approaches, and thus, are not suitable for a routine screening. Finding simple theoretical/computational tools to predict the polarity of ILs based on their individual constituent ions certainly provides significant advantages towards the rational synthesis of ILs with desired polarity for specific applications. For this reason, this work was carried out aimed at understanding the chemical structure factors affecting the hydrogen-bond acidity and polarity of ILs while foreseeing the development of a simple model for their prediction.

As a first attempt, the KT solvatochromic parameters of a wide range of $[NTf_2]$-based ILs were experimentally determined. The experimental data were then interpreted based on the major chemical structural effects governing the hydrogen-bond donating strength of ILs. Further, and aiming at providing an extended hydrogen-bond acidity scale for ILs, a reasonable correlation between the hydrogen-bond acidity values of ILs and a three-parameter model, estimated from COSMO-RS, was found. Based on this dependence, it was shown that the hydrogen-bond acidity of ILs is mostly governed by the cation–anion hydrogen-bond interactions, whereas the electrostatic-misfit and van der Waals forces also contribute, though to a lower degree. Finally, we provided a model to predict the α values of ILs, for instance for a routine screening before extensive and time-consuming experimental measurements by a trial and error approach, which opens up the possibility of pre-screening appropriate ILs (even those not yet synthesized) for a specific task or application. An extended scale for the hydrogen-bond donating ability of IL cations is also provided.

Acknowledgements

This work was developed in the scope of project CICECO – Aveiro Institute of Materials (Ref. FCT UID/CTM/50011/2013), financed by national funds through Fundação para a Ciência e a Tecnologia (FCT, Portugal)/MEC and co-financed by FEDER under the PT2020 Partnership agreement. M. G. Freire acknowledges the European Research Council (ERC) for the Grant ERC-2013-StG-337753.

References

1 J. S. Wilkes and M. J. Zaworotko, *J. Chem. Soc., Chem. Commun.*, 1992, 965–967.
2 A. M. Da Costa Lopes and R. Bogel-Lukasik, *ChemSusChem*, 2015, **8**, 947–965.
3 C. D. Tran, S. Duri, A. Delneri, M. Franko and J. Hazard, *Materials*, 2013, **252–253**, 355–366.
4 T. Welton, *Chem. Rev.*, 1999, **99**, 2071–2084.
5 V. I. Pârvulescu and C. Hardacre, *Chem. Rev.*, 2007, **107**, 2615–2665.
6 J. Brennecke and E. J. Maginn, *AIChE Annu. Meet., Conf. Proc.*, 2001, **47**, 2384–2389.
7 N. V. Plechkova and K. R. Seddon, *Chem. Soc. Rev.*, 2008, **37**, 123–150.
8 H. Passos, M. G. Freire and J. A. P. Coutinho, *Green Chem.*, 2014, **16**, 4786–4815.
9 N. V. Plechkova and K. R. Seddon, *Ionic Liquids Uncoiled – Critical Expert Overviews*, A John Wiley & Sons, Inc., Publication, 2013.
10 J. A. Laszlo and D. L. Compton, *J. Mol. Catal. B: Enzym.*, 2002, **18**, 109–120.
11 M. Gazitúa, R. A. Tapia, R. Contreras and P. R. Campodónico, *New J. Chem.*, 2014, **38**, 2611–2618.
12 C. Reichardt, *Green Chem.*, 2005, **7**, 339–351.
13 S. Spange, R. Lungwitz and A. Schade, *J. Mol. Liq.*, 2014, **192**, 137–143.
14 M. J. Kamlet, J. L. M. Abboud, M. H. Abraham and R. W. Taft, *J. Org. Chem.*, 1983, **48**, 2877–2887.
15 R. Bini, C. Chiappe, V. L. Mestre, C. S. Pomelli and T. Welton, *Org. Biomol. Chem.*, 2008, **6**, 2522–2529.
16 A. Jeličić, S. Beuermann and N. Garćia, *Macromolecules*, 2009, **42**, 5062–5072.
17 A. Jeličić, N. Garćia, H.-G. Löhmannsröben and S. Beuermann, *Macromolecules*, 2009, **42**, 8801–8808.
18 M. A. Ab Rani, A. Brant, L. Crowhurst, A. Dolan, M. Lui, N. H. Hassan, J. P. Hallett, P. A. Hunt, H. Niedermeyer, J. M. Perez-Arlandis, M. Schrems, T. Welton and R. Wilding, *Phys. Chem. Chem. Phys.*, 2011, **13**, 16831–16840.
19 P. G. Jessop, D. A. Jessop, D. Fu and L. Phan, *Green Chem.*, 2012, **14**, 1245–1259.
20 V. Znamenskiy and M. N. Kobrak, *J. Phys. Chem. B*, 2003, **108**, 1072–1079.
21 S. Pandey, S. N. Baker and G. A. Baker, *J. Fluoresc.*, 2012, **22**, 1–31.
22 R. Lungwitz and S. Spange, *New J. Chem.*, 2008, **32**, 392–394.
23 A. Schade, N. Behme and S. Spange, *Chem. – Eur. J.*, 2014, **20**, 2232–2243.
24 R. Rai and S. Pandey, *J. Phys. Chem. B*, 2014, **118**, 11259–11270.
25 A. Ali, M. Ali, N. A. Malik, S. Uzair and A. B. Khan, *J. Chem. Eng. Data*, 2014, **59**, 1755–1765.

26 A. Ali, M. Ali, N. A. Malik, S. Uzair and U. Farooq, *Fluid Phase Equilib.*, 2014, **382**, 31–41.
27 A. Ali, M. Ali, N. A. Malik and S. Uzair, *Spectrochim. Acta, Part A*, 2014, **121**, 363–371.
28 L. Kyllönen, A. Parviainen, S. Deb, M. Lawoko, M. Gorlov, I. Kilpeläinen and A. W. T. King, *Green Chem.*, 2013, **15**, 2374–2378.
29 K. Fujita, D. Kobayashi, N. Nakamura and H. Ohno, *Enzyme Microb. Technol.*, 2013, **52**, 199–202.
30 C. Chiappe, A. Sanzone, D. Mendola, F. Castiglione, A. Famulari, G. Raos and A. Mele, *J. Phys. Chem. B*, 2013, **117**, 668–676.
31 S. Zhang, Z. Chen, X. Qi and Y. Deng, *New J. Chem.*, 2012, **36**, 1043–1050.
32 A. Kobayashi, K. Osawa, M. Terazima and Y. Kimura, *Phys. Chem. Chem. Phys.*, 2012, **14**, 13676–13683.
33 S. Zhang, X. Qi, X. Ma, L. Lu and Y. Deng, *J. Phys. Chem. B*, 2010, **114**, 3912–3920.
34 V. Strehmel, R. Lungwitz, H. Rexhausen and S. Spange, *New J. Chem.*, 2010, **34**, 2125–2131.
35 S. Coleman, R. Byrne, S. Minkovska and D. Diamond, *Phys. Chem. Chem. Phys.*, 2009, **11**, 5608–5614.
36 R. Lungwitz, M. Friedrich, W. Linert and S. Spange, *New J. Chem.*, 2008, **32**, 1493–1499.
37 H. Tokuda, S. Tsuzuki, M. A. B. H. Susan, K. Hayamizu and M. Watanabe, *J. Phys. Chem. B*, 2006, **110**, 19593–19600.
38 B. R. Mellein, S. N. V. K. Aki, R. L. Ladewski and J. F. Brennecke, *J. Phys. Chem. B*, 2006, **111**, 131–138.
39 L. Crowhurst, R. Falcone, N. L. Lancaster, V. Llopis-Mestre and T. Welton, *J. Org. Chem.*, 2006, **71**, 8847–8853.
40 C. P. Fredlake, M. J. Muldoon, S. N. V. K. Aki, T. Welton and J. F. Brennecke, *Phys. Chem. Chem. Phys.*, 2004, **6**, 3280–3285.
41 S. R. Mente and M. Maroncelli, *J. Phys. Chem. B*, 1999, **103**, 7704–7719.
42 H. Niedermeyer, C. Ashworth, A. Brandt, T. Welton and P. A. Hunt, *Phys. Chem. Chem. Phys.*, 2013, **15**, 11566–11578.
43 R. Contreras, A. Aizman, R. A. Tapia and A. Cerda-Monje, *J. Phys. Chem. B*, 2013, **117**, 1911–1920.
44 A. F. M. Cláudio, L. Swift, J. P. Hallett, T. Welton, J. A. P. Coutinho and M. G. Freire, *Phys. Chem. Chem. Phys.*, 2014, **16**, 6593–6601.
45 A. Klamt and F. Eckert, *Fluid Phase Equilib.*, 2000, **172**, 43–72.
46 A. Klamt, *COSMO-RS from quantum chemistry to fluid phase thermodynamics and drug design*, Elsevier, Amsterdam, The Netherlands, 2005.
47 P. Iiiner, S. Begel, S. Kern, R. Puchta and R. Van Eldik, *Inorg. Chem.*, 2009, **48**, 588–597.
48 J. M. Lee and J. M. Prausnitz, *Chem. Phys. Lett.*, 2010, **492**, 55–59.
49 N. D. Khupse and A. Kumar, *J. Phys. Chem. B*, 2009, **114**, 376–381.
50 J.-M. Lee, *Chem. Eng. J.*, 2011, **172**, 1066–1071.
51 M. L. C. J. Moita, A. F. S. Santos, J. F. C. C. Silva and I. M. S. Lampreia, *J. Chem. Eng. Data*, 2012, **57**, 2702–2709.
52 C. M. S. S. Neves, P. J. Carvalho, M. G. Freire and J. A. P. Coutinho, *J. Chem. Thermodyn.*, 2011, **43**, 948–957.
53 J. Palomar, J. S. Torrecilla, J. Lemus, V. R. Ferro and F. Rodriguez, *Phys. Chem. Chem. Phys.*, 2008, **10**, 5967–5975.
54 J. Palomar, J. S. Torrecilla, J. Lemus, V. R. Ferro and F. Rodriguez, *Phys. Chem. Chem. Phys.*, 2010, **12**, 1991–2000.
55 University of Karlsruhe and Forschungszentrum Karlsruhe GmbH, TURBOMOLE V6.1 2009, 1989–2007, 25 GmbH, since 2007; available from http://www.turbomole.com.
56 J. B. Foresma and A. Frisch, *Exploring Chemistry with Electronic Structure Methods*, Gaussian Inc., Pittsburgh, 2nd edn, 1996.
57 F. Eckert and A. Klamt, *COSMOtherm Version C2.1 Release 01.08*, COSMOlogic GmbH & Co. KG, Leverkusen, Germany, 2006.
58 M. G. Freire, C. M. S. S. Neves, P. J. Carvalho, R. L. Gardas, A. M. Fernandes, I. M. Marrucho, L. M. N. B. F. Santos and J. A. P. Coutinho, *J. Phys. Chem. B*, 2007, **111**, 13082–13089.
59 S. P. M. Ventura, S. G. Sousa, L. S. Serafim, Á. S. Lima, M. G. Freire and J. A. P. Coutinho, *J. Chem. Eng. Data*, 2011, **56**, 4253–4260.
60 K. A. Kurnia, M. V. Quental, L. B. Santos, M. G. Freire and J. A. P. Coutinho, *Phys. Chem. Chem. Phys.*, 2015, **17**, 4569–4577.
61 P. J. Carvalho, S. P. M. Ventura, M. L. S. Batista, B. Schröder, F. Gonçalves, J. Esperança, F. Mutelet and J. A. P. Coutinho, *J. Chem. Phys.*, 2014, **140**, 064505.
62 H. Passos, A. R. Ferreira, A. F. M. Cláudio, J. A. P. Coutinho and M. G. Freire, *Biochem. Eng. J.*, 2012, **67**, 68–76.
63 K. A. Kurnia, C. M. S. S. Neves, M. G. Freire, L. M. N. B. F. Santos and J. A. P. Coutinho, *J. Mol. Liq.*, 2015, DOI: 10.1016/j.molliq.2015.1003.1040.
64 M. A. R. Martins, C. M. S. S. Neves, K. A. Kurnia, P. J. Carvalho, M. A. A. Rocha, L. M. N. B. F. Santos, S. P. Pinho and M. G. Freire, *Fluid Phase Equilib.*, 2015, DOI: 10.1016/j.fluid.2015.05.023.
65 J. N. A. Canongia Lopes and A. A. H. Pádua, *J. Phys. Chem. B*, 2006, **110**, 3330–3335.
66 M. A. A. Rocha, C. M. S. S. Neves, M. G. Freire, O. Russina, A. Triolo, J. A. P. Coutinho and L. M. N. B. F. Santos, *J. Phys. Chem. B*, 2013, **117**, 10889–10897.
67 M. A. A. Rocha, F. M. S. Ribeiro, A. I. M. C. L. Ferreira, J. A. P. Coutinho and L. M. N. B. F. Santos, *J. Mol. Liq.*, 2013, **188**, 196–202.
68 H. F. D. Almeida, M. G. Freire, A. M. Fernandes, J. A. Lopes-Da-Silva, P. Morgado, K. Shimizu, E. J. M. Filipe, J. N. Canongia Lopes, L. M. N. B. F. Santos and J. A. P. Coutinho, *Langmuir*, 2014, **30**, 6408–6418.
69 M. A. A. Rocha, C. F. R. A. C. Lima, L. R. Gomes, B. Schröder, J. A. P. Coutinho, I. M. Marrucho, J. M. S. S. Esperança, L. P. N. Rebelo, K. Shimizu, J. N. C. Lopes and L. M. N. B. F. Santos, *J. Phys. Chem. B*, 2011, **115**, 10919–10926.
70 M. A. A. Rocha, J. A. P. Coutinho and L. M. N. B. F. Santos, *J. Chem. Phys.*, 2014, **141**, 134502.
71 M. A. A. Rocha, M. Bastos, J. A. P. Coutinho and L. M. N. B. F. Santos, *J. Chem. Thermodyn.*, 2012, **53**, 140–143.
72 M. A. A. Rocha, J. A. P. Coutinho and L. M. N. B. F. Santos, *J. Phys. Chem. B*, 2012, **116**, 10922–10927.
73 M. A. A. Rocha, J. A. P. Coutinho and L. M. N. B. F. Santos, *J. Chem. Phys.*, 2013, **139**, 104502.
74 Y. Wu, T. Sasaki, K. Kazushi, T. Seo and K. Sakurai, *J. Phys. Chem. B*, 2008, **112**, 7530–7536.

